Drug Design, Development and Therapy

Dovepress
Taylor & Francis Group

Open Access Full Text Article

ORIGINAL RESEARCH

A Progesterone Microneedle Patch for Self-Administration in the Prevention of Preterm Birth in a Mouse Model

Hang Yu*, Wenting Zhu*, Zhongwen Yuan, Senling Feng, Hanhui Huang, Pengke Yan

Department of Pharmacy, Biomedicine Research Center, Guangdong Provincial Key Laboratory of Major Obstetric Diseases, Guangdong Provincial Clinical Research Center for Obstetrics and Gynecology, The Third Affiliated Hospital, Guangzhou Medical University, Guangzhou, 510150, People's Republic of China

*These authors contributed equally to this work

Correspondence: Hanhui Huang; Pengke Yan, Department of Pharmacy, Biomedicine Research Center, Guangdong Provincial Key Laboratory of Major Obstetric Diseases, Guangdong Provincial Clinical Research Center for Obstetrics and Gynecology, The Third Affiliated Hospital, Guangzhou Medical University, Guangzhou, 510150, People's Republic of China, Email hhhsimon@163.com; gysyypk@126.com

Background: Progesterone, recommended for preventing preterm birth (PTB) in high-risk women, is traditionally administered via oral capsules, vaginal gels, and oil injections, which pose issues like low bioavailability, systemic side effects, and irritation, leading to reduced compliance. To address these issues, a user-friendly administration approach to deliver progesterone was needed to development for the prevention of PTB.

Methods: We developed a progesterone microemulsion using ultra high-speed homogenization, optimizing formulation parameters and confirming stability. Subsequently, progesterone microemulsion-loaded microneedle (MN) patches were created, and its morphology, strength, and biocompatibility were assessed. The pharmacokinetics of these MN patches were then evaluated using LC/MS/MS. A mouse model was used to evaluate the therapeutic effects of the MN patch, with cell cytotoxicity, blood routine, and biochemistry tests assessing its biocompatibility.

Results: Benzyl benzoate and triglycerides were utilized as oil solvents, and Tween 80 served as the emulsifier in the preparation of a progesterone microemulsion. This formulation exhibited a particle size of 180.8 ± 20.5 nm, a zeta potential of −17.5 ± 3.4 mV, and a concentration of 20.59 ± 1.28 mg/mL. The particle size, zeta potential, and concentration of the sterilized microemulsion remained stable under 4°C. The prepared MN patch uses Povidone K30 and sucrose as excipients, which can maintain good hardness, intact needle shape, and constant drug concentration in the short term. The MN patch delivers progesterone with AUC and Cmax similar to oral progesterone microemulsion. In the preterm birth animal model, the median delivery days of mice in the progesterone microemulsion oral group and MN patch group were 19 and 20, respectively, and there was no statistical difference between the two groups. After using MN patches, the pores formed can quickly heal within 24 hours. After multiple uses of MN patches, significant abnormalities were not found in the blood routine, biochemical tests, and major organs of mice.

Conclusion: Microneedle patches loaded with progesterone microemulsion were successfully developed, efficiently delivering progesterone and reversing RU486-induced preterm birth in mice. The MN patch was user-friendly, minimally harmful to skin tissue, safe, and non-toxic, representing a promising new approach for the clinical treatment of premature labor.

Keywords: progesterone, preterm birth, microneedle, transdermal delivery, self-administration

Introduction

Preterm birth (PTB) is the leading cause of adverse pregnancy outcomes.[1] According to the World Health Organization, over 15 million premature infants are born each year, accounting for more than 10% of all births.[2] PTB is a syndrome induced by multiple factors, including luteal phase defects, inflammation/infection, immune dysregulation, and cervical insufficiency.[3] Notably, luteal phase defects (LPD) account for the highest number of PTBs. LPD occur when the corpus luteum produces

Received: 20 November 2024
Accepted: 8 March 2025
Published: 1 April 2025

Graphical Abstract

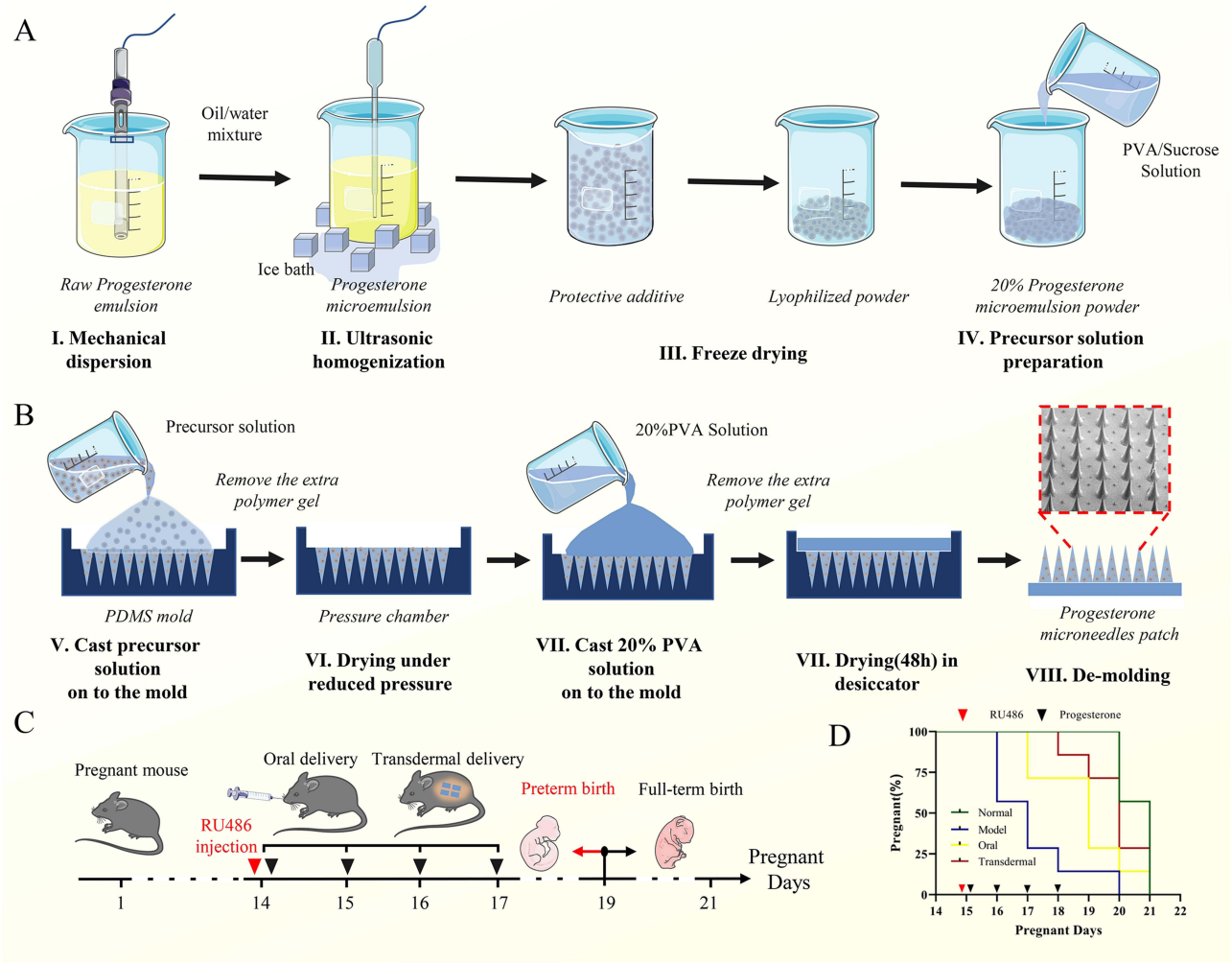

insufficient progesterone or the luteal phase is too short, leading to problems with pregnancy implantation and support.[4] In clinical practice, exogenous progesterone supplementation is commonly administered to pregnant women identified as being at high risk for PTB.[5] As a result, progesterone-based therapies have been extensively researched for the prevention of PTB. Traditionally, progesterone has been delivered via oral tablets, capsules, vaginal gels, and injection forms.[6,7]

Due to first-pass effects and gastrointestinal digestive enzymes, oral administration of progesterone required higher oral doses to achieve an effective therapeutic concentration.[8] This led to high oral doses and serious systemic side effects.[9] Vaginal progesterone had been used for more than 20 years to support luteal function and early pregnancy after assisted reproduction.[10] But the vaginal delivery formulation of progesterone almost always liquefies and leak immediately once applied at body temperature, which could be messy and also lead to a loss of active drug.[10] At the same times, the frequently use of vaginal gel always resulted to the vaginal irritation and epithelial toxicity. The negative impacts always result patient compliance and limit the therapeutic outcomes. Intramuscular injection of progesterone is administered for a variety of indications, including preterm birth.[11] Nevertheless, intramuscular injection requires a trained person for administration and it becomes difficult for women to go to the clinic every day for another injection which leads to discontinuation.[12] Additionally, the absorption of progesterone from oil preparation after injected transdermal is not complete and delayed to fulfill the rapid therapy effect, which also tend to produce local induration.[13] The inconvenient delivery method of intramuscular injection of progesterone oil drawback the benefits of therapy.[11]

Consequently, there is a growing interest in developing a more convenient and cost-effective method for progesterone delivery. Transdermal delivery facilitates the permeation of therapeutically effective amounts of drugs across the skin, allowing them to enter systemic circulation. This method serves as an alternative route to oral and parenteral administration of drugs.[14,15] As a new type of transdermal drug delivery technology, microneedles (MNs) have aroused great interest among numerous scientists since its proposal in the 1870s and have used in drug delivery in 1998. MNs consist of micron-scale projections, creating temporary channels for delivering active pharmaceutical agents into systemic circulation, which could improve the drug bioavailability, enhance drug sustained release, minimize adverse reaction and improve the pharmacological responses of active ingredients.[16,17] Due to their limited length of 50–1000 μm, MNs do not reach nerve endings, providing the advantage of administering various types of drugs, such as proteins,[18] DNA/RNA[19] and vaccines,[20] using a noninvasive and pain-free approach without influence by the physical properties of the drug. Lee et al reported on a self-administered MN patch designed for long-acting contraception. This patch utilized poly-(lactic-co-glycolic acid) MNs to gradually release the contraceptive hormone levonorgestrel over a duration of up to 1 month. In addition, the MNs could separate from the patch with 1 min and remain embedded under the skin surface after patch removal because the special backing of the MN patch containing sodium bicarbonate and citric acid that effervesces upon application to skin and contact with the skin's interstitial fluid.[21] Gomaa et al developed a thermostable oxytocin MN patch, which enabled rapid delivery of oxytocin and was suitable for use by healthcare workers with limited training. Oxytocin was coated onto stainless steel MN arrays by physical absorption with only 10IU, 16.8 μg, which had no significant loss for up to 2 months in 40°C at 75% relative humidity.[22] However, the stability of oxytocin was assessed by HPLC, no pharmacokinetic or pharmacologic researches were executed to evaluated in vivo absorption and confirm that the pharmacotherapeutic efficacy. In addition, this type of microneedle is limited by the special principle of adsorption drug loading, and cannot deliver the required amounts of active gradients that need high dosage to fulfill therapeutic purposes. These studies inspire us to construct a progesterone delivery microneedle with sustained release effects that can maintain stable drug levels, while using appropriate animal models to investigate its therapeutic efficacy.

Although the small size of MN patches was beneficial, they typically had a limited drug dosage capacity of sub-milligram levels.[23] Efforts were practiced to address these problems; He et al prepared an MN incorporating inclusion complexes loaded with progesterone; Phuvamin et al loading progesterone microemulsion into microneedles; however, only in vitro characterization was conducted, which could not provide an actual pharmacotherapies efficiency of the drug delivery system and the patch size was too large to be suitable to the patient.[14,24] Consequently, achieving an effective dosage and stable level of progesterone in plasma via transdermal delivery presents significant challenges for the clinical application of progesterone MN patches.

In this study, we developed a microemulsion-based MN patch to deliver an efficient dosage of progesterone to systemic circulation whereas achieving sustained release, as depicted in Scheme 1. The preparation methods and physicochemical characteristics of the progesterone microemulsion and MN patch are detailed in this article. Moreover, biosafety assessments, including the evaluation of key organ function and skin recovery capability, demonstrated that the MN patch exhibited good biocompatibility. Collectively, the self-administered MN patch provides a simple and convenient method for the sustained delivery of progesterone, which has the potential to enhance access to progesterone support for women and reduce the rate of PTB.

Materials and Methods

Progesterone was obtained from Macklin, Inc. (Shanghai, China). Triglycerides and benzyl benzoate were purchased from Sigma-Aldrich (St. Louis, MO, USA). PVP K30, polyvinyl alcohol (PVA), polyoxymethylene hydrogenated castor oil, poloxamer 407, and soybean lecithin were sourced from Macklin Inc. (Shanghai, China). Mannitol, sucrose, lactose, glucose, and trehalose were obtained from Macklin Inc. (Shanghai, China). Dialysis bags with a 100 kDa molecular weight cutoff were acquired from Thermo Scientific™ (MA, USA). RU486 (mifepristone) was also purchased from Macklin Inc. (Shanghai, China).

Animals

Female C57BL/6 mice (6–8 weeks) and healthy Sprague-Dawley (SD) rats (200–250 g) were purchased from BesTest Bio-Tech (Zhuhai, China) and kept in SPF environment. All animal studies were performed in accordance with the legal

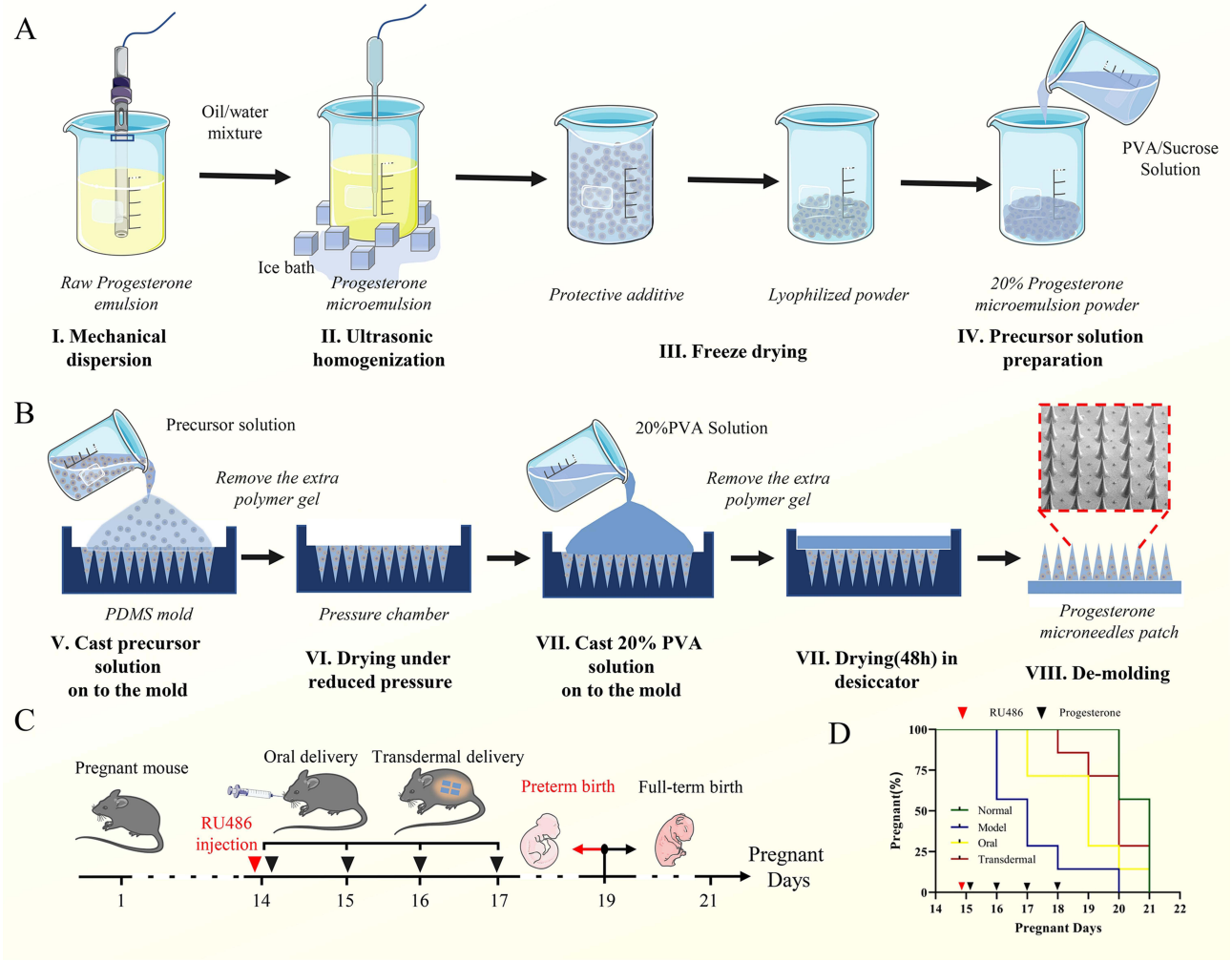

Scheme 1 Schematic figures of a self-administrated progesterone microneedle patch for the effective treatment of preterm birth in mice. (**A**) Preparation procedure of progesterone microemulsion powder; (**B**) Fabrication process of progesterone microneedles patch; (**C** and **D**) Progesterone microneedles patch fulfilled an effective efficacy to the preterm birth induced by RU486.

mandates and national guidelines for the care and maintenance of laboratory animals. The Ethics Committee of the Third Affiliated Hospital of Guangzhou Medical University approved all experimental protocols (Code: 2023–071).

Preparation of Progesterone Microemulsion

The fabrication process for the progesterone microemulsion is depicted in Scheme 1A. In summary, the oil phase consisting of 0.8 g of progesterone, 0.96 g of soybean oil, 4 g of triglyceride, and 4 g of benzyl benzoate was prepared in a 50 mL beaker. The aqueous phase, containing 2 g of glycerin and 0.072 g of sodium oleate, was heated separately to 75°C. We supplied the method for determining the solubility of progesterone in different solvents in Supplement materials methods section 1.1. A high-speed homogenizer (Kinematica B, Switzerland) was employed to emulsify the oil and aqueous phases at 75°C with 14000 rpm for 1 min and repeated 3 times. Subsequently, the raw emulsion was then homogenized in the ice bath using an ultrasonic probe to yield the progesterone microemulsion, the relative parameters was fixed as follows, 200W was applied, with 55 cycles of a 3 s sonication and a 3 s pause. The emulsion was then homogenized in the ice bath using an ultrasonic probe to yield the progesterone microemulsion. Finally, a 1 M NaOH solution was utilized to adjust the pH of the microemulsion to between 9.5 and 10. The microemulsions were packaged in 5 mL amber ampoules and sterilized at 115°C for 20 min. The resulting solutions were stored at 4°C in a dark environment. To produce a high-concentration progesterone MN patch, the microemulsion was freeze-dried to obtain

a powder. We practiced a series of protectants with different components (Table S1) and selected the best one which keep the microemulsion stable after freeze-drying process with good apparent of the powder. Additionally, Dir loaded microemulsions were prepared using the same method, with minor modifications, substituting progesterone with 40 μL of Dir (50 mg/mL) for the visualization of the MN.

Characterization of Progesterone Microemulsion

The Zetasizer (Zeta Sizer nano-ZS90, Malvern, UK) was utilized to determine the size, size distribution, and zeta potential of the microemulsion droplets. The microemulsion was diluted 10 times using ultra-pure water as the working solution for the measurement of size and zeta potential at 25 ± 2 ◦C and 90◦ scattering angle, and each sample was analyzed three times. All samples were stored at 4°C, and the particle size, potential, concentration and other parameters of progesterone microemulsion were measured, respectively, at 0,24,48,72,96 h. The pH of the microemulsion samples was measured using pH paper.

Fabrication of Progesterone MN Patch

The preparation of the progesterone MN patch using the templating method is illustrated in Scheme 1B. Initially, we used three sizes of microneedle templates to prepare microneedle patches (Table S2), namely small (15.8 mm * 15.8 mm), medium (16.7 mm * 16.7 mm), and large (29 mm * 29 mm). And the poly dimethyl siloxane (PDMS) mold featuring MNs with a conical structure (base radius of 300 μm, height of 800 μm) arranged in a 20×20 array across an area of 16.7 mm by 16.7 mm and center-to-center spacing of 700 μm, the medium one, was utilized for fabricating the progesterone microemulsion MN patch through a negative pressure technique.

To create the progesterone MN patches, two solutions, casting and backing, were prepared and applied sequentially to the mold. Initially, 100 μL of the MN casting solution, comprising PVA/sucrose (10%, w/v, 1:1) dissolved in a progesterone microemulsion (80 mg/mL), was introduced into the mold cavities. In some instances, the MN casting solution included a 100 μg/mL DIR microemulsion to enhance imaging capabilities. Subsequently, the mold was placed in an oven at 25°C under pressurized air (0.2 MPa) for 3 min. Any residual solution on the surface was scraped off using a glass coverslip and collected for later use. Another 100 μL of the casting solution was then added to the mold cavities and dried. This loading and drying process was repeated five times. The casting solution was ultimately dried completely in a glass desiccator containing anhydrous silica gel for 3 days.

Following this, a backing solution composed of 10% PVA and 10% PVP K30 was prepared and applied to the upper surface of the mold. The filling of the backing solution was executed under negative pressure using the same procedure as before, followed by a drying period of 2 days at room temperature in a desiccator. The final progesterone MN patches were stored in a desiccator at room temperature until needed and were subsequently removed from the mold using medical adhesive tape.

A series of mixtures, incorporating progesterone microemulsions, saccharides, and polymer materials, were prepared separately to optimize the formulation of the progesterone MN patches. The polymer materials, which included PVA, PVP, chitosan, sodium hyaluronate, along with saccharides (sucrose, glucose, trehalose, and dextran), were dissolved in the progesterone microemulsion. Only the optimized formulations of the progesterone MN patches are discussed here. 2–3 patches were randomly test for progesterone content and particle size in each batch of prepared patches to ensure the quality of the samples. The manufactured progesterone MN patches contained 600 μg of progesterone per patch and were subsequently used for both characterization of the preparation and follow-up animal studies. All patches were used in 1 week after prepared.

Characterization of Progesterone MN Patch

Confocal microscopy (Nikon, A1R+N-STORM, Tokyo, Japan) was employed to assess the surface morphology of patches containing either progesterone or Nile red. Scanning electron microscopy (SEM, FEI Tecnai G2 F20 S-Twin 200Kv, US) facilitated the observation of the morphology of the MN arrays coating with gold according Sun et al.[25] The MNs were dispersed in deionized water, applied to a copper grid, and subsequently dried at room temperature to analyze the morphology of the progesterone microemulsion incorporated into the MNs using a transmission electron microscope

(TEM, JEOL, JEM 1400 PLUS, Tokyo, Japan) according Dixon et al.[26] The structural characteristics of pure progesterone, the corresponding microemulsion, and the MN patches were verified using a Fourier-transform infrared (FTIR) spectrophotometer (Nicolet iS50, Thermo Scientific, USA) with 64 scans for samples and the transmittance was evaluated in wave number from 4000 to 400 cm^{-1}, with 4 cm^{-1} resolution according Qasim et al.[27] X-ray diffractometer (XRD) analysis of pure progesterone, the associated microemulsion, and the MN patches was conducted with an X-ray diffractometer (Rigaku ULTIMA IV, Japan) equipped with Cu Kβ radiation, a power of 3 kW. The samples were scanned in a range of 0–40° in a continuous mode with a scanning rate of 10°/min.

Mechanical Characterization and Penetration Capacity of Progesterone MN Patch

The microneedle patch was inserted into a tightly adhered four layers aluminum foil using a customized injection device and then removed from the aluminum foil.[28,29] Four layers of aluminum foil paper were spread onto an A4 paper, and applying blue ink on the surface of the aluminum foil paper. The ink can penetrate into the A4 paper through the perforations caused by microneedles and leave ink marks. Microneedles with different mechanical hardness can penetrate different layers of aluminum foil, so the number of perforations on different layers of aluminum foil is also different, resulting in different amounts of ink left on A4 paper. By separately counting the number of ink marks left by blue ink on A4 paper, the mechanical hardness and puncture ability of the microneedle can be indirectly reflected.

In Vitro Release Behaviors of Progesterone From MN Patch

Modified Franz diffusion cells were utilized to investigate the in vitro release behaviors of progesterone from MN patch according Andi et al.[30] A piece of skin from rat abdominal skin was practiced for the in vitro release. The subcutaneous adipose tissue and hair of the skin were carefully removed using a surgical knife and washed with pure water. The processed skin was sealed in a plastic without fold and stored in −20°C. A circular piece of the processed skin was thawed at room temperature and secured on the PBS fulfilled Franz diffusion cell with the stratum corneum facing the donor compartment for 1 h to hydrate it before conducting in vitro release study. MNs, prepared by different size template, containing varying amounts of progesterone were inserted into the upper surface of the skin using a customized injection apparatus. Medical adhesive tape was used to anchor the MN patches in place over the upper surface of the skin. The receptor compartments of the Franz cells contained 0.25% Tween 80 in phosphate-buffered saline (PBS). At predetermined intervals of 0,4,6,12,24,48,72,96 h, samples were collected from the receptor compartment and replaced with an equal volume of PBS. High-performance liquid chromatography (HPLC; 1260 Infinity, Agilent, Japan) was employed to determine the concentration of progesterone in the samples. A Diamonsil C18 column (250 × 4.6 mm, 5 μm pore size) (Dikma Technologies Inc., USA) was used at 25°C to detect the drug content. The mobile phase was methanol: acetonitrile: water (43:40:17) with a 1mL/min flow rate and the prog was detected at 8.6 min under 256.4 nm wavelength.

In Vivo Pharmacokinetics of Microemulsion From MN Patch

Dir-loaded MN patches were applied to the abdominal skin of healthy C57BL/6 mice to study the delivery ability of microneedle patch, twelve mice were given free access to water and food and randomly divided to two groups (n = 6) as small and medium patch. Following the administration of the dissolvable MNs, the mice were imaged at a predetermined time of 0 h, 1h, and 3 h using a small-animal live optical imaging system (IVIS Lumina HTX, PerkinElmer, USA). Radiant efficiency was measured to evaluate the transdermal effectiveness of the MNs and the biodistribution of progesterone (Prog) in the abdominal skin.

Healthy Sprague-Dawley (SD) rats weighing 200–250 g was applied to evaluate the pharmacokinetic of the progesterone delivered by microneedle patch. The abdominal fur of was removed with depilatory cream and allowed to recover for 24 h. The rats of the control group were orally administrated with equivalent dose of progesterone microemulsion. Whole blood was collected from the posterior vena orbitalis at predetermined time points and centrifuged at 4000 rpm for 10 min to collect plasma. The concentrations of Prog were analyzed using HPLC-MS/MS (API3200MD, AB SCIEX, USA) followed the instruction as Supplement materials methods section 1.2. The resulting plasma concentration-time curve was plotted, with C_{max} defined as the maximum plasma concentration of Prog. T_{max} was identified as the time at which Prog reached C_{max},

whereas $t_{1/2}$ was the time at which C_{max} decreased to half its value. The area under the concentration-time curve from zero to the time of the last quantifiable concentration was designated as AUC_{0-t}.

Therapeutic Potency of Progesterone MN Patch in Preterm Birth Mice Model

To verify the therapeutic potency of progesterone Mn patch, we built a progesterone withdrawn resulted preterm birth mice model. Forty pregnant mice were housed in cages 7 days prior to experiments. On the morning of gestation day 15 (E15), ten mice were separated with other as the normal group and other mice received a subcutaneous injection of RU486, a progesterone antagonist dissolved in DMSO, at a dose of 25 μg to induce PTB, in the scruff of the neck. Subsequently, the PTB mice were randomly divided into three groups (n = 10) and ten pregnant mice were included in each group. The PTB mice were treated with Prog via different administration methods-oral (2.60 mg/kg) or transdermal (4.06 mg/kg) to study the efficacy of luteal support provided by Prog MN patches. This administration regimen was continued daily each morning until E18, totaling four treatments. Staff who have no conflict of interest with this study conduct the drug administration procedure until the end of the experiment. The occurrence of at least one fetal delivery within 24 h of RU486 injection at E15 was classified as PTB, whereas live births occurring after the morning of E19 were classified as delivery at term. 12 h post-RU486 injection, the cervices of half of the mice were collected and fixed in formalin solution for 24 h. These specimens were then embedded in paraffin, sectioned longitudinally, and stained with Masson's trichrome.

Biosafety Assays

Vascular epithelial cells (VSMC, purchased from FengHuiShengWu) were seeded in 96-well plates and culture in 1640 medium with 10% fetal bovine serum (FBS, Procell Life Science&Technology Co., Ltd) for 24 h in a humidified incubator at 37°C containing 5% CO_2. The cytotoxic effect of different progesterone concentrations of pure progesterone, progesterone microemulsion, precursor of progesterone microneedle and corresponding blank carriers, respectively, on VSMC was detected by MTT assay after the co-incubation of 48 h. The absorbance at 490 nm was measured using a microplate apparatus (BioTek, Vermont, UK).

Prior to the skin tissue recovery experiment, the backs of the SD rats were shaved using an animal hair removal cream (Veet®) and divided to three groups: normal group without MN treated, other two groups were treated with progesterone microneedle patch and the skin tissue samples were collected at either 0 h or 24 h post-application after rat euthanasia. Six SD rats were included in each group. The acquired skin tissue treated with MNs was stored in formalin (10% v/v). The skin samples were sectioned and stained with hematoxylin and eosin following standard histological staining procedure. The tissue slides were examined under various magnifications using a microscope to assess biosafety.

Following treatment with progesterone, the principal organs of the PTB mouse model were collected after the administration of MNs and stained with hematoxylin and eosin to ensure the biosafety of the MN patches. Furthermore, whole blood samples were obtained and processed to conduct routine blood tests and biochemistry analysis using an Exigo automatic blood analyzer (Boule, Sweden).

Statistical Analysis

Data was expressed as the mean ± standard deviation and were analyzed using analysis of variance (ANOVA) followed by Tukey's multiple comparison in GraphPad Prism 8 and the sample sizes were equal (or nearly so) in all experiments. Log rank test (Mantel-Cox) was done for all three curves in GraphPad Prism 8 testing the null hypothesis that all the samples come from populations with the same survival and that differences are due to chance. Multiple comparisons of the median day of parturition using pairwise comparisons between two administration groups and normal or model group was also done in Graphpad Prism 8. Statistical significance is indicated by multiple asterisks, where $*P < 0.05$, $**P < 0.01$, and $***P < 0.001$.

 https://doi.org/10.2147/DDDT.S502701

Results and Discussion

Preparation of Progesterone Emulsion

Although the transdermal MN patch presents a convenient method for drug delivery, it also has inherent limitations, such as low drug loading, which becomes particularly challenging with high doses of commonly used drugs like progesterone. The characteristic volume of a dissolvable MN is typically 10 nL, meaning that a patch containing 100 MNs can hold a maximum of 1 μg of the active pharmaceutical ingredient if the precursor has a concentration of 1 mg/mL for the drug.[23] More importantly, the amount of drug constitutes only a small fraction of the MN materials, necessitating the use of a substantial quantity of excipients to ensure the mechanical strength of the MNs and enable dissolution.[31] Additionally, progesterone is a poorly water-soluble drug with low transdermal delivery efficiency, bioavailability, and clinical dosages in the milligram range.[32] Consequently, various strategies have been employed in designing the progesterone MN transdermal patch, including increasing the drug concentration in the precursor, reducing the proportion of excipients, and enlarging the size of the MN patch.

We prepared a microemulsion formulation that significantly enhances the solubility of drugs. During the preparation of the microemulsion, as illustrated in Scheme 1A, we selected various types and ratios of oil solvents to optimize the drug loading capacity of the progesterone microemulsion. The solubility of progesterone in benzyl benzoate was determined to be 240.3 ± 21.5 mg/mL, as shown in Figure S1. However, due to the irritant nature of benzyl benzoate during intramuscular injection, we limited its maximum dosage to 50% in accordance with FDA guidelines. We then explored the solubility of progesterone in a mixture of benzyl benzoate and soybean oil/triglyceride. Our findings revealed that a 1:1 volume ratio of triglyceride to benzyl benzoate significantly enhanced progesterone solubility; therefore, we selected this ratio for the oil phase.

Concurrently, we evaluated various surfactants by analyzing changes in particle size and zeta potential during short-term storage of the microemulsion. Figure 1A–D demonstrate that a progesterone microemulsion prepared with 1 mg/mL Tween 80 as the surfactant exhibited excellent particle size and zeta potential stability over 130 h, with an average particle size of 180.8 ± 20.5 nm and a potential of −17.5 ± 3.4 mV. The sterilization conditions had a notable impact on the physical stability of the 10 mg/mL progesterone emulsion. Specifically, sterilization at 121°C for 15 min resulted in an increase in emulsion size (Figure 1E), whereas a lower temperature condition of 115°C for 30 min did not affect the size or zeta potential stability of the progesterone emulsion (Figure 1G). Similar results were observed for the 20 mg/mL progesterone emulsion (Figure 1F–H). In order to acquire stable progesterone emulsion, we practiced sterilization procedure under 115°C for 15 min. Finally, we assessed the changes in particle size, zeta potential, and concentration of both types of microemulsions over a 30-day storage period before and after sterilization. The results indicated that after autoclaving at 115°C for 30 min, the particle size, zeta potential (Figure 1I and J), and concentration (Figure 1K) of the progesterone microemulsion remained stable. We chose 10% PVP K30 as the cryoprotectant of the progesterone microemulsion because good apparent of the drying powder (Figure S2). In conclusion, the progesterone microemulsion developed in this study demonstrates favorable potential, as well as stability in terms of particle size and concentration.

Preparation of Prog MNs Patches

The preparation process for the Prog MNs patches is illustrated in Scheme 1B. The composition and proportions of the MN matrix were examined to develop a progesterone MN transdermal patch that maintained the integrity of the needle shape, demonstrated sufficient strength, and achieved high drug loading. To enhance drug loading, we utilized 80 mg/mL of Prog ME and 5% PVA as polymer materials. The stability and strength of the MNs were enhanced by incorporating a specific proportion of sucrose. To assess the effect of sucrose content on the penetrating ability and strength of the MNs, we conducted puncture tests on multilayer aluminum foil using the MN patches, thereby determining the optimal sucrose concentration. As depicted in Figure 2A, there was an increase in the number of punctured layers of aluminum foil with higher sucrose content in the MNs. Figure 2B reveals that when sucrose content in the MNs reached 20%, the perforation rate for the third layer of aluminum foil was 62% ± 10%. Although further increases in sucrose content could enhance the MN puncture intensity, the improvements were marginal. Consequently, we established the progesterone MN matrix at 20% sucrose, 5% PVA, and 80 mg/mL Prog ME.

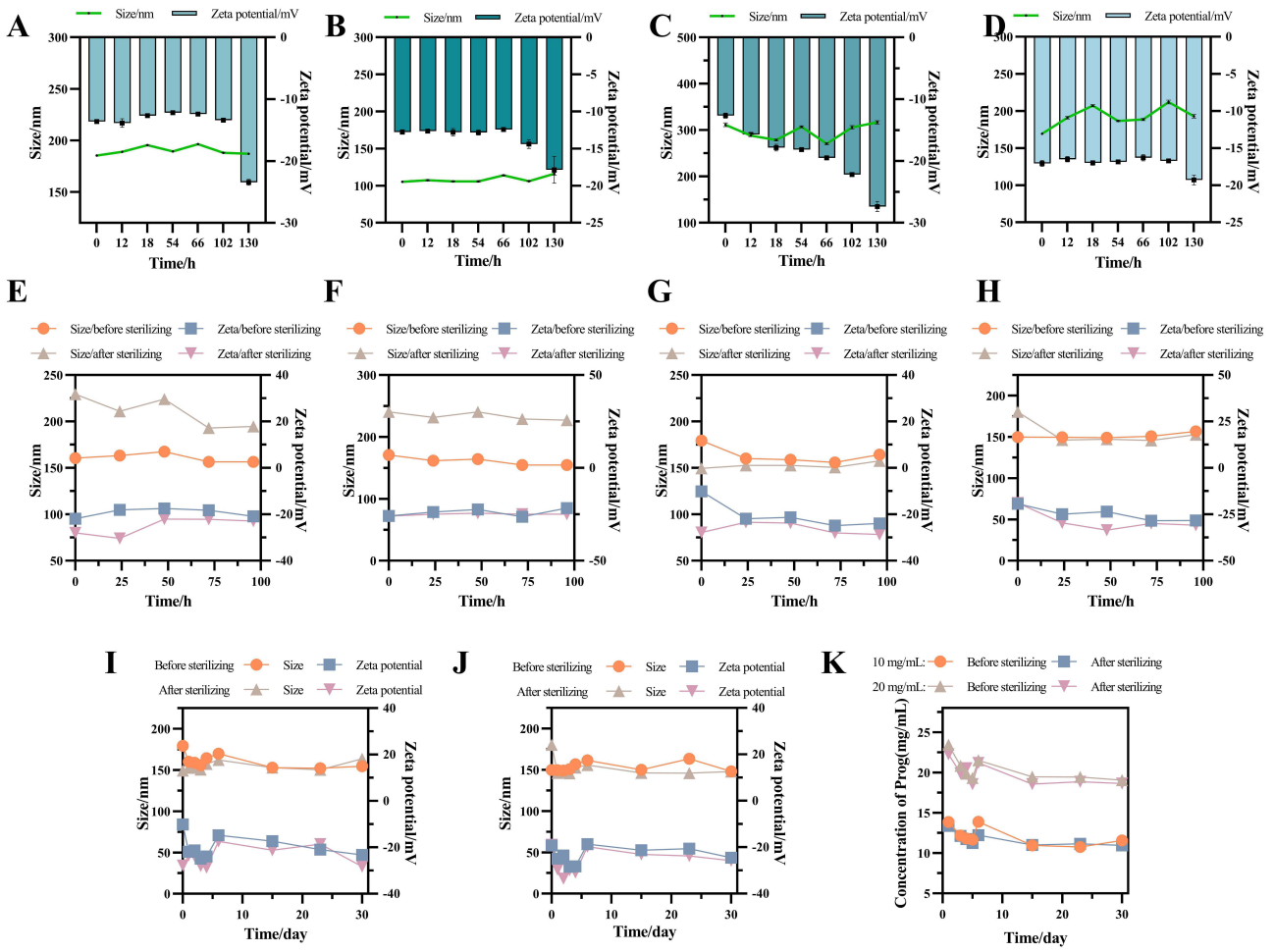

Figure 1 Size and zeta potential changes of progesterone emulsion emulsified by soybean lecithin (**A**), Poloxamer 188 (**B**), Cremophor EL (**C**) or Tween 80 (**D**). Size and zeta potential changes 10 mg/mL (**E**) and 20 mg/mL (**F**) progesterone microemulsion sterilized under 121°C for 15 min. Size and zeta potential changes of 10 mg/mL (**G**) and 20 mg/mL (**H**) progesterone microemulsion sterilized under 115°C for 30 min. Long term size and zeta potential changes of 10mg/mL (**I**) or 20mg/mL (**J**) progesterone microemulsion. Concentration changes of progesterone emulsion (**K**).

To optimize the progesterone content in the MN patches, we explored MN templates of various sizes (small, medium and large). The actual progesterone content in the MN patches did not significantly differ from the anticipated theoretical value, which presumes the absence of excipients (Figure 2C). However, excipients constitute a considerable portion of the volume. This discrepancy may be attributed to the concentration of the precursor during the drying phase of MN preparation. Additionally, the primary drug content in the large-sized MN patch deviated notably from the theoretical value, likely due to the uneven distribution of the MN matrix liquid across the larger template area during preparation. We employed a modified diffusion cell method to evaluate the in vitro transdermal release capabilities of the three MN patches (Figure 2D). The findings indicated that the medium-sized MN patch released its drug within 48 h, accounting for only 53.3%±4.6% of the drug load. In contrast, the small-sized MN patch achieved complete release after 96 h, with a release rate of 37.5% ± 4.2%. The large-sized MN patch released 60.4%±6.9% of its drug content within 96 h. Although the small-sized MN patch exhibited a slower drug release rate, it failed to load a higher dose of progesterone compared with the medium-sized MN patch. The drug released content across the three MN patch sizes adhered to the same trend as the actual content found in the MN patches. Therefore, we did not pursue further investigation of the large-sized MN patches.

Furthermore, we investigated the content changes of the two sizes of MN patches over a 28-day period and found that their drug content stabilized at 400 μg (418.13 ± 50.07) and 600 μg (591.88 ± 60.63), respectively, on day 28. This

https://doi.org/10.2147/DDDT.S502701

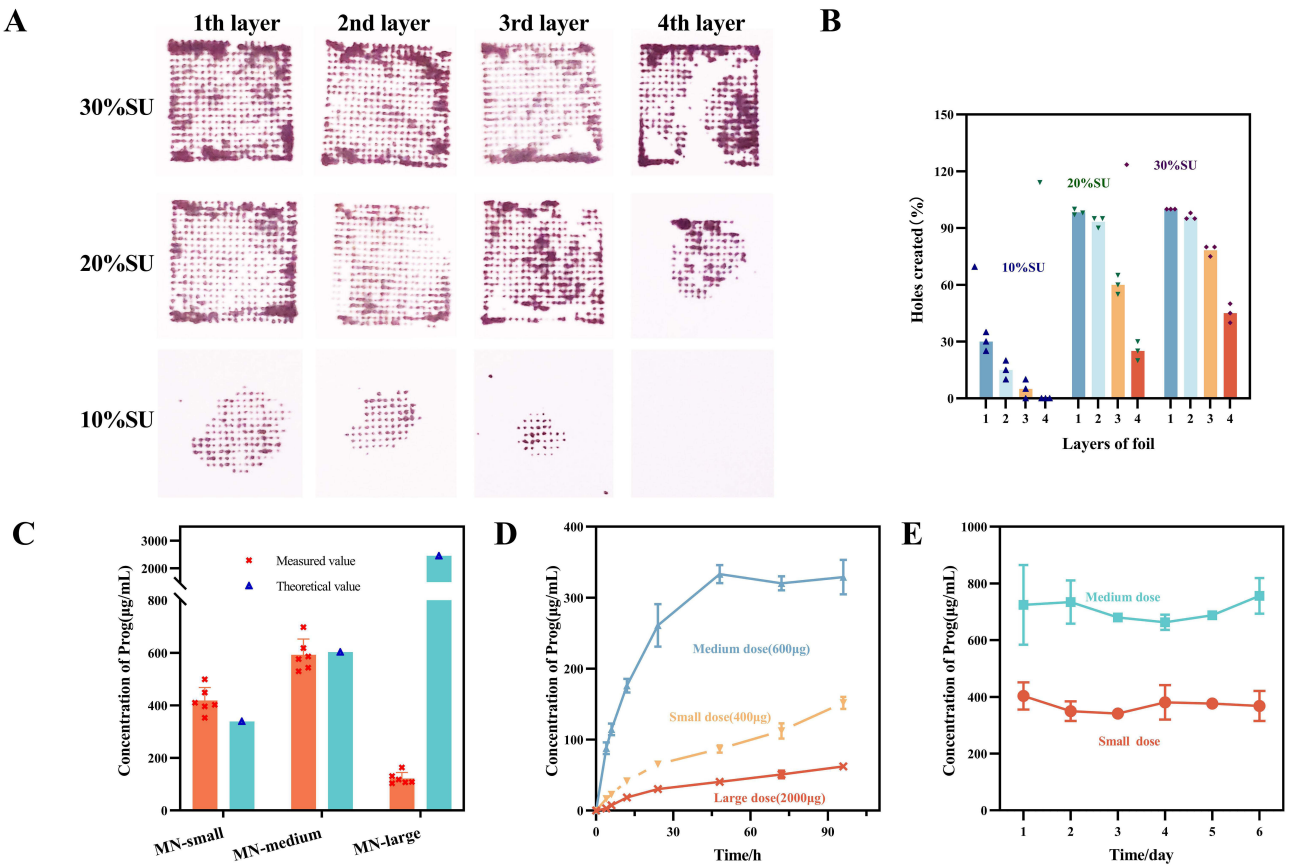

Figure 2 Images of Ink dots in the A4 papers (**A**) reflected the holes in different layers created by different content of sucrose of the progesterone MNs. The quantitative data of holes created by MNs in different layers of foil (**B**). Concentration of progesterone in MNs with different sizes (**C**). Progesterone release curve of progesterone from MNs with different dimensions (**D**). The concentration changes of progesterone in MNs (**E**).

indicates the stability of progesterone within the MN patches (Figure 2E). To support luteal function in cases of premature births in mice, we selected a medium-sized MN patch containing 600 μg of progesterone for a follow-up study.

Characterization of Progesterone Microemulsion and MNs Patches

We characterized the physical properties of both the progesterone microemulsion and the MN patches. TEM images revealed that the progesterone microemulsion was uniform and regularly spherical (Figure 3A), with an average particle size of 85 ± 7 nm. SEM images of the prepared MN patch (Figure 3B) confirmed that the MNs were conical, consistent with the shape of the MN template. This characteristic was also observed in the optical microscopy images (Figure S3A) and fluorescence images (Figure S3B) of the MN patches. The hydrated particle size of the progesterone microemulsion was measured at 130 nm ± 1.5 nm (Figure 3C), which was larger than the true particle size observed in the TEM image. The hydrated particle size reflects the combined diameter of the particle core plus the surrounding water phase, whereas the TEM sample depicts the true particle size after the removal of the outer water phase from the particle core.[33] This discrepancy was related to the detection principles of TEM and had no influence on the characteristic of our progesterone microemulsion. The zeta potential of the progesterone microemulsion was recorded at 25.6 ± 1.8 mV (Figure 3D). Given that the progesterone microemulsion utilized PVA as a stabilizer, this charge level assists in preventing the aggregation of particles, maintaining their stability.[34] This conclusion was corroborated by the preparation of the progesterone MN patch. As illustrated in Figure 3E, the particle sizes of the progesterone emulsion, lyophilized powder, MN matrix solution, and MN patch exhibited relative uniformity and stability in potential. The results indicated that the stability of the progesterone microemulsion particles was preserved despite decompression, cooling, or heating during the MN preparation process.

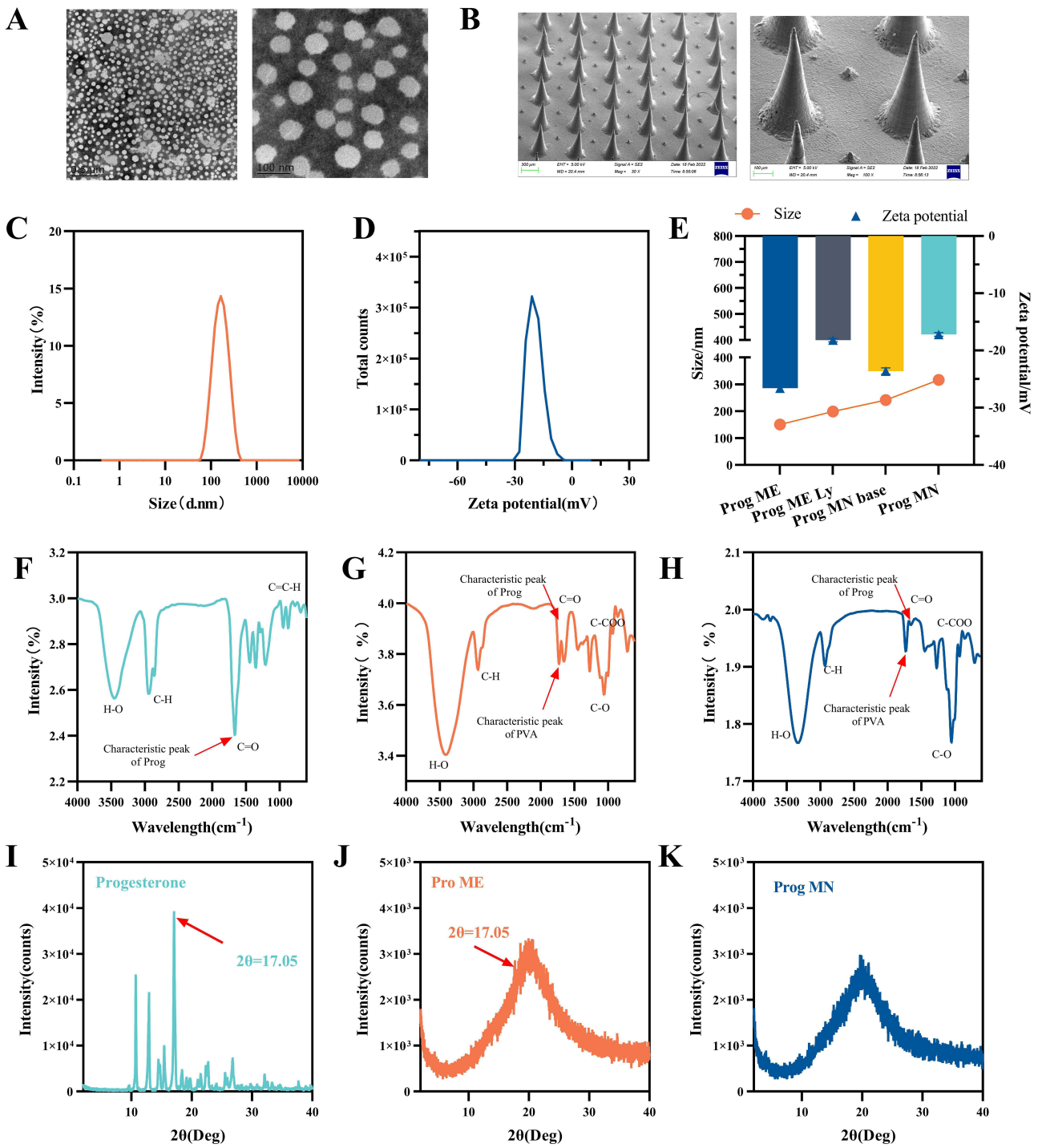

Figure 3 TEM images (**A**) of progesterone emulsion under different magnifications. SEM images (**B**) of progesterone MNs under different magnifications. Size (**C**) and zeta potential (**D**) diagrams of progesterone emulsion. Size and zeta potential changes (**E**) of different progesterone preparations. FTIR diagrams of progesterone (**F**), progesterone emulsion (**G**) and progesterone MNs (**H**). XRD diagrams of progesterone (**I**), progesterone emulsion (**J**) and progesterone MNs (**K**).

In the infrared absorption spectrum of the raw progesterone material (Figure 3F), we observed a pronounced characteristic absorption peak of progesterone at 1700 cm^{-1}. This characteristic absorption peak was also present in the infrared absorption spectra of both the lyophilized powder of the progesterone microemulsion (Figure 3G) and the MN patch (Figure 3H). Additionally, the O-H stretching vibration absorption peak at 3300 cm^{-1} and the C-O stretching vibration absorption peak at 1150 cm^{-1} corresponded to the PVA polymer. The X-ray diffraction (XRD) patterns

https://doi.org/10.2147/DDDT.S502701

(Figure 3I) demonstrated that both the progesterone microemulsion (Figure 3J) and the MN patch (Figure 3K) possessed amorphous structures, fundamentally differing from crystalline progesterone.

Pharmaceutical Kinetics of Prog Administrated by MNs Patch

In this study, we employed a Dir microemulsion instead of a progesterone microemulsion to evaluate the efficacy of the MN patch during transdermal administration. An in vivo imaging system was utilized to monitor changes in the radiation efficiency of Dir over time (Figure 4A). The results demonstrated that the MN patch rapidly dissolved in the skin of mice, with the drug concentration on the skin surface peaking at 1 hour before gradually declining (Figure 4B). The concentration of the drug delivered by small- and medium-sized patches was found to be correlationally associated with the drug load. Notably, the radiation efficiency of Dir in the medium MN patch group was significantly higher than that observed in the small MN patch group.

Additionally, we explored the pharmaceutical kinetics of progesterone administered via MN patches. Given that the progesterone preparation was exogenous and the detection method employed was unable to differentiate between endogenous and exogenous progesterone, we conducted pharmacokinetic experiments using healthy male mice to eliminate the potential interference of endogenous progesterone fluctuations on the reliability of the experimental results.[29,30] The plasma dynamics of progesterone following intragastric administration (Figure 4C and D) and administration via the MN patch (Figure 4E and F) indicated that the drug time profile for progesterone exhibited a double peak following the administration of the progesterone microemulsion. However, this double peak was absent after the administration of the progesterone MN patch, which may indicate a slower release profile associated with the MN patch. Key parameters of the drug time profile are summarized in Table 1; the time to peak (9 h) and the half-life (6 h) for the progesterone MN patch were postponed compared to the oral progesterone group. Nevertheless, the area under the drug curve at both 24 h and 72 h was comparable, suggesting that the progesterone released from the MN patch occurred more smoothly than that from oral administration whereas maintaining similar bioavailability. This finding aligns with

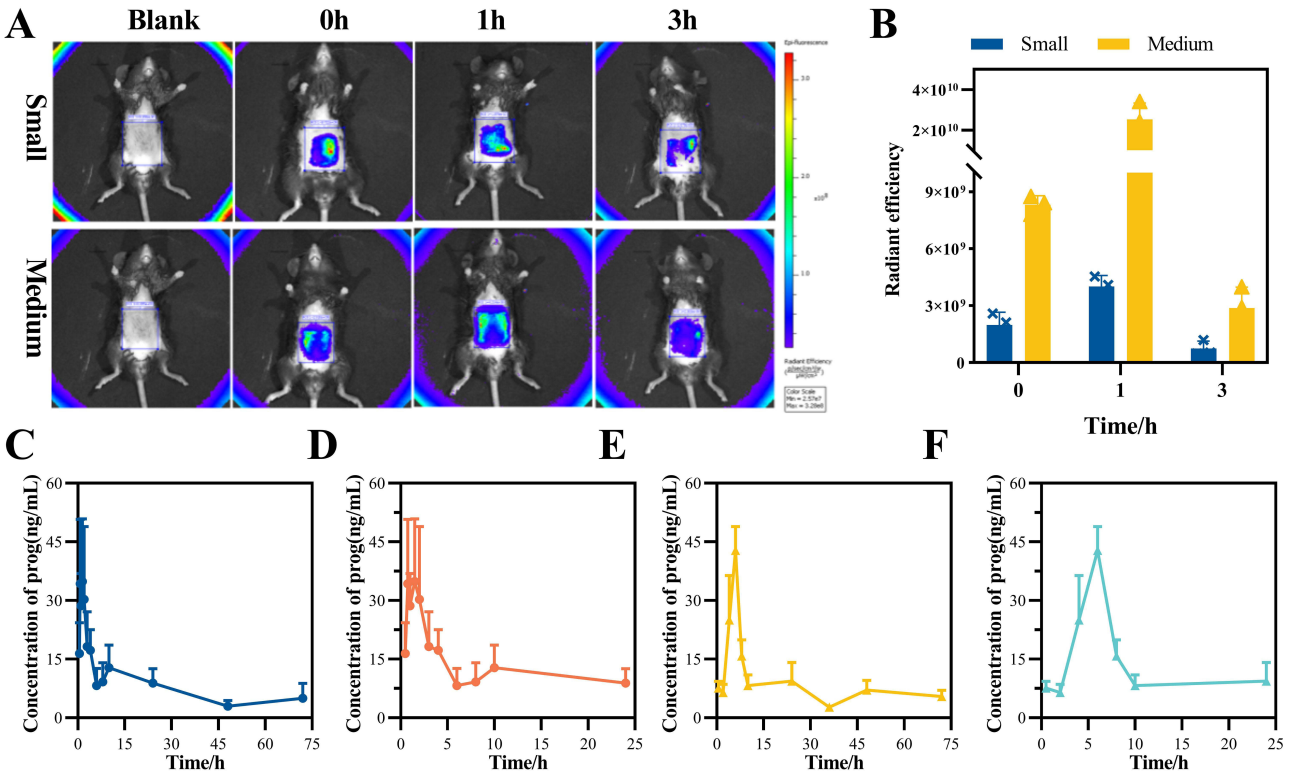

Figure 4 In vivo radiant imaging of mice administrated with Dir MNs patches (**A**) and corresponding data analysis (**B**). Plasma progesterone concentration versus time curve in the healthy SD mice administrated by oral (**C**) for 72h, (**D**) for 24h) and transdermal (**E**) for 72h, (**F**) for 24h) approach.

Table 1 Pharmaceutical Kinetics Parameters of Progesterone (Means ± S.D., n = 5)

Parameter	Oral	MNs
$t_{1/2}$(h)	3	9
T_{max}(h)	1.5	6
C_{max}(ng/mL)	34.84±16.01	42.81±6.09
AUC_{0-72}(ng/mL*h)	542.2±85.93	597.7±64.88
AUC_{0-24}(ng/mL*h)	304.9±51.77	315.9±43.22

trends observed in in vitro transdermal drug diffusion experiments, further indicating that MN transdermal delivery of progesterone can sustain a stable blood drug concentration.

Therapeutic Efficacy of Prog MNs Patches to RU486 Induced Preterm Birth

Both ovariectomy and the administration of the progesterone antagonist to pregnant mice resulted in reduced progesterone production, leading to cervical remodeling and preterm delivery. In contrast, exogenous progesterone supplementation has been shown to maintain a normal pregnancy.[35,36] The initiation of labor in mice is associated with the binding of progesterone to its receptors. Mifepristone (RU486), as a competitive antagonist of progesterone, binds to progesterone receptors in vivo, thereby inducing labor.[37] For the first time, Dudley et al established a functional progesterone withdrawal animal model using mifepristone.[35] Additionally, T. Hoang et al proposed that exogenous progesterone supplementation could counteract PTB caused by low doses of mifepristone. Their findings demonstrated that an 8 mg dose of exogenous progesterone administered via vaginal gel could reverse 85% of PTBs induced by 25 μg of mifepristone furtherly.[38] Vieira et al developed progesterone-loaded waterborne polyurethane-urea nanocomposite membranes, which exhibited the ability to penetrate the skin barrier and control progesterone release.[39] Furthermore, the progesterone inclusion MNs prepared by He et al using PVA and hydroxypropyl cellulose demonstrated good mechanical strength and effectively delivered progesterone directly to the skin, achieving a higher transdermal delivery volume.[40] However, studies on the percutaneous delivery of progesterone have primarily been limited to in vitro experiments, which do not fully capture the benefits of this approach in the treatment of PTB. To address this gap, we established an RU486-induced PTB mouse model to assess the efficacy of luteal support administered via a progesterone MN transdermal patch.

The therapeutic efficacy of the experimental process was illustrated in Figure 5A. On day 15 of gestation (E15), mice received subcutaneous injections of RU486 in the neck, whereas progesterone was administered both orally and transdermally to provide luteal support over a continuous 4-day period. As shown in Figure 5B, the rate of PTB in untreated pregnant mice was zero, with the median delivery occurring on the 21st day of pregnancy. In the PTB model group, delivery occurred on the second day following RU486 injection, resulting in an 80% incidence of preterm delivery, with a median delivery day of 17. Following oral progesterone treatment, the pregnancy maintenance rate in the treated mice was 75%, with the median delivery day recorded at 19. This represented a statistically significant difference compared to the normal group ($p < 0.01$, Table 2) though no significant difference was observed compared to the model group. In contrast, the PTB rate in the progesterone MN patch treatment group was significantly lower at just 20%, with a median delivery day of the 20th day, which also displayed a significant difference compared to the model group ($p < 0.01$, Table 2). These results indicate that both the progesterone MN patch and progesterone microemulsion can effectively counteract RU486-induced PTB in mice and delay the onset of labor. Notably, the normal pregnancy rate among mice administered the MN patch was higher than that of mice treated with the oral microemulsion, potentially due to the stable progesterone blood concentration achieved in the MN patch group.

On the 18th day of gestation, the uteri of select mice were dissected, and the tissues were collected for paraffin embedding, sectioning, and Masson staining. The uteri of mice in the model group exhibited a dark coloration and reduced length, suggesting the occurrence of stillbirth and myometrial contractions. No significant differences were noted between the uteri of mice receiving luteal support and those in the normal group. At the conclusion of gestation, the

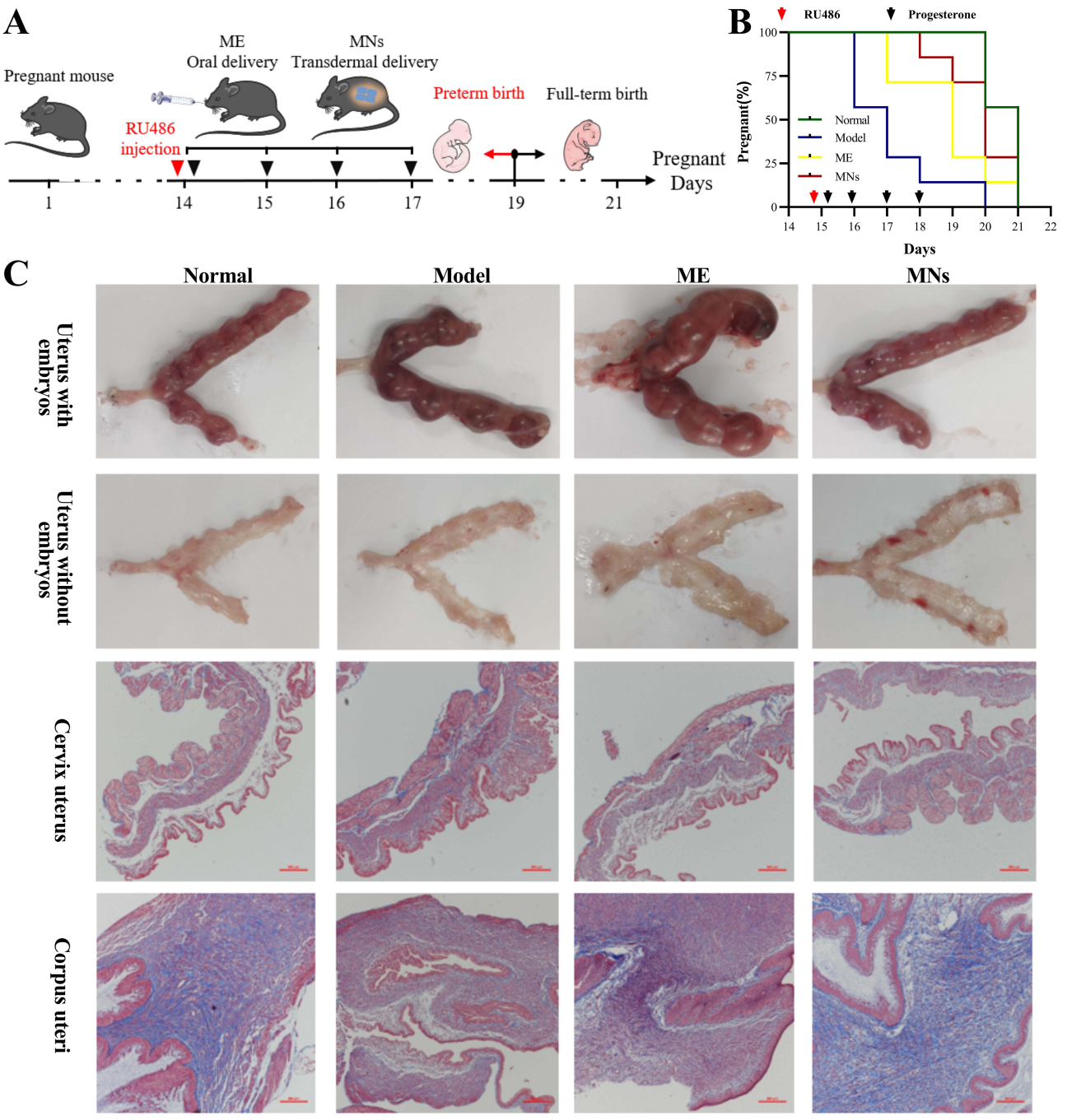

Figure 5 Therapeutic potency of progesterone microneedle patch in preterm birth mice model. Scheme diagram of model building and therapy regime (**A**). Percentage of animals remaining pregnant after RU486 injection on E15 out of a total gestation of 19 days (**B**). Images of uterus with/without embryos and corresponding pathological section images stained with Masson's Trichrome(**C**).

cervix softened, and the birth canal underwent remodeling in preparation for labor. A key characteristic of cervical softening is the dispersal of collagen, as confirmed by Masson's trichrome staining of the cervix.[41,42] Masson staining revealed a decrease in collagen staining and an increase in collagen spacing in the model group (Figure 5C), whereas no differences in collagen staining intensity were observed between the normal group and both treatment groups.[43] Following treatment with a progesterone MN patch, the PTB induced by RU486 in mice was averted, suggesting a novel avenue for research into progesterone drug delivery methods.

Table 2 Multiple Pairwise Comparison Log-Rank p value

Groups	Median Day of Parturition	P values Compared to Normal	P values Compared to Model
Normal	21	–	0.0008(***)
Model	17	0.0008(***)	–
Oral	19	0.0191(**)	0.0639(ns)
MN	20	0.1762(ns)	0.0069(**)

Notes: Data is Presented as Average ± SE for n = 4–5 Mice per Time Point. ns Means No Significant Differences,* $p < 0.05$, ** $p < 0.01$, and *** $p < 0.001$.

The physiological secretion of progesterone is a continuous process.[36,44] The concentration of progesterone in females is typically maintained at levels between 0.14 and 0.7 ng/mL during a normal physiological cycle. However, this level can increase twenty-fold during pregnancy, returning to normal levels after delivery.[45,46] Specifically, in pregnant mice, the progesterone concentration remains stable throughout the pregnancy and declines at the end of gestation to facilitate the onset of labor.[47,48] To effectively mimic the physiological secretion of endogenous progesterone, exogenous progesterone supplementation must create a stable pharmacokinetic profile within the circulation system.[7,49,50] However, the rapid absorption and elimination of progesterone following oral administration can hinder its effectiveness as a treatment for premature birth, potentially leading to significant systemic side effects, such as dizziness and sleep disorders in patients.[12,46] In contrast, utilizing an MN patch for progesterone delivery can effectively slow the absorption and elimination processes, ensuring a more stable blood concentration. Given the prolonged treatment duration required for exogenous progesterone supplementation, the development of a long-acting, slow-release transdermal patch is both clinically valuable and appealing.

In clinical practice, premature birth was a syndrome caused by multiple factors, and the specific mechanism of occurrence was still unclear.[51] There were many reasons for premature birth, including infection, stress, placental abruption, and mechanical pressure.[36] Among numerous animal premature birth models, hormone models played an important role, and the premature birth model induced by progesterone receptor antagonist RU486 was the most typical non inflammatory premature birth model in mice.[52] The mechanism of action of this animal model was closely related to endocrine regulation, and our research mainly focused on using microneedle patches to supplement exogenous progesterone, thereby antagonizing premature birth in animals caused by RU486. Therefore, our drug delivery system had certain reference significance for the therapy of premature birth caused by endocrine disorders. Future research should focus on enhancing the drug-loading capacity of the MN patch with the characteristic of controlled drug release rate post-administration by a more convenient preparation procedure.

Biosafety of Prog MNs Patches

Results from the cytotoxicity analysis demonstrated that the blank microemulsion at a low concentration exhibited no cytotoxic effects (Figure 6A), whereas high concentrations of the progesterone raw material did not impact cell viability. The toxicological effects observed from the progesterone microemulsion and the progesterone MN patch were comparable to those of the progesterone raw material, suggesting that the progesterone MN patch possesses favorable biocompatibility.

We investigated the recovery circumstance of the rat abdominal skin treated with a progesterone MN patch. As illustrated in the results (Figure 6B), we could obviously observe a conical wound, indicated by the red arrow, in the cuticle of the skin tissue immediately after application of MN patch (0 h) in the image of the skin section slide. Simultaneously, the wound was disappeared within 24 h after the application, which indicated that the channels created by the MN administration on the skin surface closed quickly and did not result in any permanent damage.

Histological examination through HE staining of the principal organs, including the liver, spleen, and kidneys, revealed normal morphology, with no evident pathological changes (Figure 6C). The routine blood and biochemical indices of the mice following multiple administrations of progesterone preparations showed no significant differences

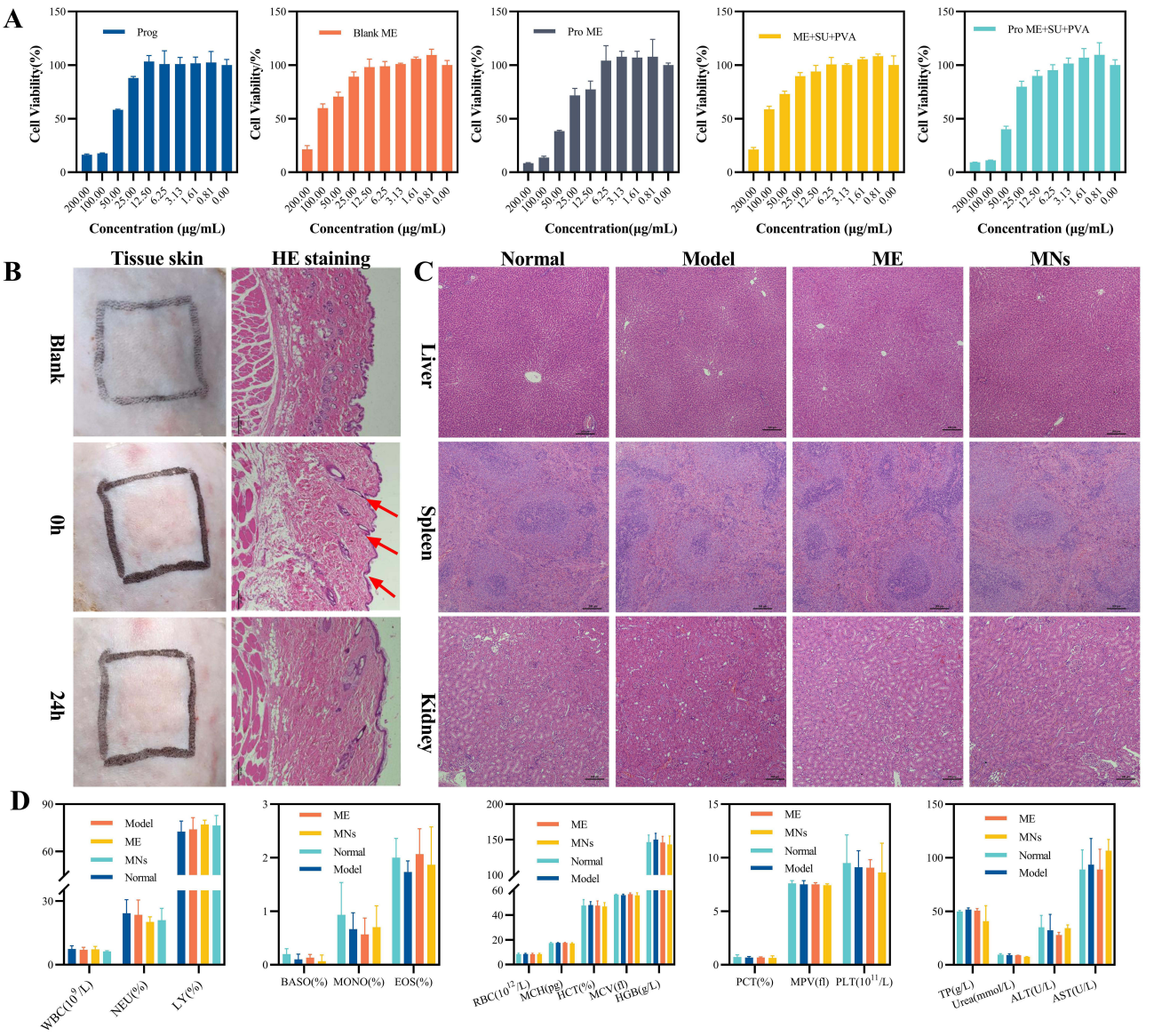

Figure 6 Biocompatibility of progesterone preparations. Cytotoxicity of progesterone preparations proved by cell viability of VSMC (**A**). Skin recovery after administrated with MNs patches reflected by the HE images of skin tissue sectioned slide (**B**). HE images of main organs (**C**). Blood routine and blood biochemistry data (**D**).

compared to those in the control group, indicating that the progesterone MN patch did not induce hepatorenal toxicity in the animals (Figure 6D).

Conclusion

This study developed a stable, high-capacity microemulsion for enhanced progesterone delivery in MN patches. Different MN substrates were tested for their impact on patch hardness, resulting in an effective transdermal patch with robust delivery capabilities. The progesterone MN patch proved effective in treating RU486-induced PTB in mice and showed relative safety. Overall, the MN patch is user-friendly, minimally invasive to the skin, safe, and non-toxic, offering a promising approach for treating premature labor clinically.

Acknowledgments

This work was supported by the Natural Science Foundation of Guangdong Province (No. 2025A1515011942), Guangzhou Health Technology General Guidance Project (20221A011094), Plan on enhancing scientific research in

GMU (2025SRP023), Research Fund Project of the Third Affiliated Hospital of Guangzhou Medical University (2020Q09), Guangdong Basic and Applied Basic Research Foundation (2024A03J0189, 2024A03J0188), Guangdong Medical Research Foundation (B2023154, A2024212), Research Project of Guangdong Provincial Administration of Traditional Chinese (20241181) and Guangzhou Municipal Bureau of Science and Technology Key Research and Development Program (2024B03J0056).

Author Contributions

All authors made a significant contribution to the work reported in the conception, study design, execution, acquisition of data, analysis and interpretation; took part in drafting, revising or critically reviewing the article; gave final approval of the version to be published; have agreed on the journal to which the article has been submitted; and agree to be accountable for all aspects of the work.

Disclosure

The authors declare no conflicts of interest.

References

1. Krispin E, Hessami K, Johnson RM, et al. Systematic classification and comparison of maternal and obstetrical complications following 2 different methods of fetal surgery for the repair of open neural tube defects. *Am J Clin Exp Obstet Gynecol*. 2023;229(1):53.e1–53.e8.
2. New World Health. Organization recommendations for care of preterm or low birth weight infants: health policy. *EClinicalMedicine*. 2023;63:102155.
3. DeTomaso A, Kim H, Shauh J, et al. Progesterone inactivation in decidual stromal cells: a mechanism for inflammation-induced parturition. *Proc Natl Acad Sci USA*. 2024;121(25):e2400601121.
4. Garg A, Zielinska AP, Yeung AC, et al. Luteal phase support in assisted reproductive technology. *Nat Rev Endocrinol*. 2024;20(3):149–167.
5. Shynlova O, Nadeem L, Lye S. Progesterone control of myometrial contractility. *J Steroid Biochem mol Biol*. 2023;234:106397.
6. Kabiri D, Hamou Y, Gordon G, Ezra Y, Matok I. Comparing the efficacy of vaginal micronized progesterone gel and capsule for prevention of preterm birth in singleton pregnancies with short cervical length at midtrimester: an indirect comparison meta-analysis. *Front Pharmacol*. 2023;14:1153013.
7. Cao Z, Tang X, Zhang Y, et al. Novel injectable progesterone-loaded nanoparticles embedded in SAIB-PLGA in situ depot system for sustained drug release. *Int J Pharm*. 2021;607:121021.
8. Niu Y, Liu H, Li X, et al. Oral micronized progesterone versus vaginal progesterone for luteal phase support in fresh embryo transfer cycles: a multicenter, randomized, non-inferiority trial. *Human Reproduction*. 2023;38(Supplement_2):ii24–ii33.
9. Maheshwari R, Bhatt LK, Wairkar S. Enhanced oral bioavailability of progesterone in bilosome formulation: fabrication, statistical optimization, and pharmacokinetic study. *Am J Clin Exp Obstet Gynecol*. 2024;25(2):29.
10. Tran VTT, Nguyen NA, Nguyen NT, et al. Development of children born to women with twin pregnancies treated with cervical pessary or vaginal progesterone: follow-up of a randomized controlled trial. *Acta obstetricia et gynecologica Scandinavica*. 2023;102(5):626–634.
11. Salem HF. Sustained-release progesterone nanosuspension following intramuscular injection in ovariectomized rats. *Int J Nanomed*. 2010;5:943–954.
12. Patil N, Maheshwari R, Wairkar S. Advances in progesterone delivery systems: still work in progress? *Int J Pharm*. 2023;643:123250.
13. Hibbard T, Shankland K, Al-Obaidi H. Preparation and formulation of progesterone para-aminobenzoic acid co-crystals with improved dissolution and stability. *Eur J Pharm Biopharm*. 2024;196:114202.
14. He H, Wang Z, Aikelamu K, et al. Preparation and in vitro characterization of microneedles containing inclusion complexes loaded with progesterone. *Pharmaceutics*. 2023;15:6.
15. Patil P, Vankani A, Sawant K. Design, optimization and characterization of atorvastatin loaded chitosan-based polyelectrolyte complex nanoparticles based transdermal patch. *Int J Biol Macromol*. 2024;274(Pt 1):133219.
16. Yang J, Yang J, Gong X, et al. Recent progress in microneedles-mediated diagnosis, therapy, and theranostic systems. *Adv Healthcare Mater*. 2022;11(10):e2102547.
17. Liu H, Zhou X, Nail A, et al. Multi-material 3D printed eutectogel microneedle patches integrated with fast customization and tunable drug delivery. ***J Control Release***. 2024;368:115–130.
18. Li L, Zhao Z, Yang X, et al. A newly identified spike protein targeted linear B-cell epitope based dissolvable microneedle array successfully eliciting neutralizing activities against SARS-CoV-2 wild-type strain in mice. *Advanced Sci*. 2023;10(20):e2207474.
19. You Y, Tian Y, Yang Z, et al. Intradermally delivered mRNA-encapsulating extracellular vesicles for collagen-replacement therapy. *Nat Biomed Eng*. 2023;7(7):887–900.
20. Wang H, Xu J, Xiang L. Microneedle-mediated transcutaneous immunization: potential in nucleic acid vaccination. *Adv Healthcare Mater*. 2023;12(23):e2300339.
21. Lee Y, Li W, Tang J, Schwendeman SP, Prausnitz MR. Immediate detachment of microneedles by interfacial fracture for sustained delivery of a contraceptive hormone in the skin. ***J Control Release***. 2021;337:676–685.
22. Gomaa Y, Kolluru C, Milewski M, et al. Development of a thermostable oxytocin microneedle patch. ***J Control Release***. 2021;337:81–89.
23. Li W, Li S, Fan X, Prausnitz MR. Microneedle patch designs to increase dose administered to human subjects. ***J Control Release***. 2021;339:350–360.
24. Suriyaamporn P, Aumklad P, Rojanarata T, et al. Fabrication of controlled-release polymeric microneedles containing progesterone-loaded self-microemulsions for transdermal delivery. *Pharmaceu Develop Technol*. 2024;29(2):98–111.

25. Sun B, Zhang T, Chen H, et al. Microneedle delivery system with rapid dissolution and sustained release of bleomycin for the treatment of hemangiomas. *J Nanobiotechnol*. 2024;22(1):372.
26. Dixon RV, Skaria E, Lau WM, et al. Microneedle-based devices for point-of-care infectious disease diagnostics. *Acta Pharmaceutica Sinica B*. 2021;11(8):2344–2361.
27. Cui X, Shu H, Wang L, et al. Methacrylic functionalized hybrid carbon nanomaterial for the selective adsorption and detection of progesterone in wastewater. *Environ Sci Pollut Res Int*. 2021;28(44):62306–62320.
28. Trinh VL, Chung CK. A facile method and novel mechanism using microneedle-structured PDMS for triboelectric generator applications. *Small*. 2017;13:29.
29. Wu X, Chen Y, Gui S, et al. Sinomenine hydrochloride-loaded dissolving microneedles enhanced its absorption in rabbits. *Pharmaceu Develop Technol*. 2016;21(7):787–793.
30. Permana AD, Paredes AJ, Volpe-Zanutto F, Anjani QK, Utomo E, Donnelly RF. Dissolving microneedle-mediated dermal delivery of itraconazole nanocrystals for improved treatment of cutaneous candidiasis. ***Eur J Pharm Biopharm***. 2020;154:50–61.
31. Le Z, Yu J, Quek YJ, et al. Design principles of microneedles for drug delivery and sampling applications. *Mater Today*. 2023;63:137–169.
32. Zhang Y, Zhang R, Illangakoon UE, et al. Copolymer composition and nanoparticle configuration enhance in vitro drug release behavior of poorly water-soluble progesterone for oral formulations. *Int J Nanomed*. 2020;15:5389–5403.
33. Wilson BK, Prud'homme RK. Nanoparticle size distribution quantification from transmission electron microscopy (TEM) of ruthenium tetroxide stained polymeric nanoparticles. *J Colloid Interface Sci*. 2021;604:208–220.
34. Li J, Guo P, Hu C, et al. Fabrication of large aerogel-like carbon/carbon composites with excellent load-bearing capacity and thermal-insulating performance at 1800 °C. *ACS Nano*. 2022;16(4):6565–6577.
35. Dudley DJ, Branch DW, Edwin SS, Mitchell MD. Induction of preterm birth in mice by RU486. *Biology Repro*. 1996;55(5):992–995.
36. Zierden HC, Shapiro RL, DeLong K, Carter DM, Ensign LM. Next generation strategies for preventing preterm birth. *Adv Drug Delivery Rev*. 2021;174:190–209.
37. Gorenberg D, Beharry K, Nishihara KC, et al. Dose response of RU486 in a novel rabbit model of noninfectious preterm birth: comparative efficacy of 3 routes of administration. *Am J Clin Exp Obstet Gynecol*. 2005;192(3):924–931.
38. Hoang T, Zierden H, Date A, et al. Development of a mucoinert progesterone nanosuspension for safer and more effective prevention of preterm birth. ***J Control Release***. 2019;295:74–86.
39. Vieira IRS, Costa LDFDO, Miranda GDS, et al. Transdermal progesterone delivery study from waterborne poly(urethane-urea)s nanocomposites films based on montmorillonite clay and reduced graphene oxide. *J Drug Delivery Sci Technol*. 2020;60:101873.
40. Romero R, Conde-Agudelo A, Da Fonseca E, et al. Vaginal progesterone for preventing preterm birth and adverse perinatal outcomes in singleton gestations with a short cervix: a meta-analysis of individual patient data. *Am J Clin Exp Obstet Gynecol*. 2018;218(2):161–180.
41. Malik M, Roh M, England SK. Uterine contractions in rodent models and humans. *Acta Physiologica*. 2021;231(4):e13607.
42. Moghaddam AO, Lin Z, Sivaguru M, et al. Heterogeneous microstructural changes of the cervix influence cervical funneling. *Acta Biomater*. 2022;140:434–445.
43. Collins A, Motiwale T, Barney O, Dudbridge F, McParland PC, Moss EL. Impact of past obstetric history and cervical excision on preterm birth rate. *Acta obstetricia et gynecologica Scandinavica*. 2021;100(11):1995–2002.
44. Ashoush S. Oral micronized progesterone is effective for preventing preterm delivery. *Acta obstetricia et gynecologica Scandinavica*. 2020;99 (3):427–428.
45. Stewart LA, Simmonds M, Duley L, et al. Evaluating progestogens for preventing preterm birth international collaborative (EPPPIC): meta-analysis of individual participant data from randomised controlled trials. *Lancet*. 2021;397(10280):1183–1194.
46. Piette PCM. The pharmacodynamics and safety of progesterone. *Best Pract Res Clin Obstet Gynaecol*. 2020;69:13–29.
47. da Fonseca EB, Damião R, Moreira DA. Preterm birth prevention. *Best Pract Res Clin Obstet Gynaecol*. 2020;69:40–49.
48. Raghupathy R, Szekeres-Bartho J. Progesterone: a unique hormone with immunomodulatory roles in pregnancy. *Int J Mol Sci*. 2022;23:3.
49. Wang M, Liu M, Xie T, Zhang BF, Gao XL. Chitosan-modified cholesterol-free liposomes for improving the oral bioavailability of progesterone. *Colloids Surf B*. 2017;159:580–585.
50. Memi E, Pavli P, Papagianni M, Vrachnis N, Mastorakos G. Diagnostic and therapeutic use of oral micronized progesterone in endocrinology. *Rev Endocr Metab Disord*. 2024;25(4):751–772.
51. Goldenberg RL, Culhane JF, Iams JD, Romero R. Epidemiology and causes of preterm birth. *Lancet*. 2008;371(9606):75–84.
52. Shynlova O, Nadeem L, Dorogin A, Mesiano S, Lye SJ. The selective progesterone receptor modulator-promegestone-delays term parturition and prevents systemic inflammation-mediated preterm birth in mice. *Am J Clin Exp Obstet Gynecol*. 2022;226(2):249.e1–249.e21.